Wiley Online Library
Early View publication on www.wileyonlinelibrary.com
(issue and page numbers not yet assigned;
citable using Digital Object Identifier – DOI)

Phys. Status Solidi B, 1–6 (2014) / DOI 10.1002/pssb.201451268

physica status solidi b
www.pss-b.com
basic solid state physics

Band-gap and phonon distribution in alkali halides

I. S. Messaoudi[1], A. Zaoui*[,2], and M. Ferhat[1]

[1] Département de Physique., Université des Sciences et de la Technologie d'Oran, USTO, Oran, Algeria
[2] LGCgE, Ecole Polytechnique de Lille, Université des Sciences et de la Technologie de Lille, Cité Scientifique, Avenue Paul Langevin, 59655 Villeneuve D'Ascq Cedex, France

Received 1 June 2014, revised 3 September 2014, accepted 25 September 2014
Published online 21 October 2014

Keywords alkali halides, band-gap, computational physics, density functional theory, phonons, thermodynamics

* Corresponding author: e-mail azaoui@polytech-lille.fr, Phone/Fax: 00 3 20 43 46 13

A systematic first-principles study is performed to calculate the structural, electronic, dynamical, and thermodynamic properties of alkali halides NaF, NaCl, NaBr, and NaI by means of both full-potential linear augmented plane-wave, and plane wave pseudopotential methods. The obtained structural parameters agree favourably with experimental findings. The calculated band gaps are underestimated by GGA functional compared to experiment. The gap values are improved from the modified Becke–Johnson exchange potential, which gives band gaps in perfect agreement with the measured values. In addition, linear-response approach to the density functional theory is used to derive several quantities such as the Born effective charges, high-frequency dielectric constant, phonon band structure, and phonon density of states. The dynamical properties of Na-based alkali halides are also analysed and discussed. Finally the temperature dependence of various quantities such as the mean-squared displacement, and the heat capacity are computed using the quasi-harmonic approximation.

1 Introduction Alkali halides NaX [X is element of group VII (F, Cl, Br, I)] are the simplest and most representative ionic crystals. The pioneering work of Madelung and Ewald [1] has opened the way to explore the chemistry and physics of alkali halides. The alkali halides NaF, NaCl, NaBr, and NaI crystallize in the rocksalt (B1) structure at ambient conditions, and they are distinguished by a large variety of interesting physical properties such as high melting points, strong miscibility, and large band gaps. Moreover alkali halides find technological use as infrared (IR) optical windows, and optoelectronic devices.

Besides several optical measurements that elucidate the electronic structure of NaX compounds, first-principles calculation can help to investigate their electronic and optical properties. However the density functional theory (DFT) [2] calculations within the local density approximation (LDA) [3] or generalized gradient approximation (GGA) [4] give rise to a typical underestimation of electronic excitation energies, such as energy gaps. For instance, the calculated [5–6] lowest band gaps are severely underestimated compared to experiment. This is the case of calculated LDA band gaps [5] of 7.26, 6.38, 5.84, and 4.37 eV for NaF, NaCl, NaBr, and NaI, respectively, compared to the measured values [7] of 11.5, 8.75, 7.1, and 5.9 eV.

There are only few reports on the dynamical properties [8–11] of the NaX compounds. Most of them used the empirical models, such as modified shell model, a deformable shell model and three-body-force shell model. These models fit the experimental phonon dispersion curves at the cost of adjustable parameters (10 or more), which have no physical interpretation. Moreover, to the best of our knowledge, no further theoretical data based on first-principles calculation of the dynamical and thermodynamic properties are available to date. An accurate description of the vibrational properties of solids is crucial, as they play a significant role in determining various materials properties such as the structural phase transition, electron–phonon interaction, thermodynamic stability, transport and thermal properties.

Our main message here will be threefold: (i) to present a systematic study of the structural, electronic, dynamical and thermodynamic properties of NaF, NaCl, NaBr, and NaI compounds; (ii) to improve the band gaps of these materials from those calculated previously; (iii) to get an accurate

description of the lattice dynamics and related properties of alkali halides using DFT and linear-response approach to the DFT.

The rest of the paper is organized as follows: in Section 2, we briefly describe the computational techniques used in this work. Results and discussions will be presented in Section 3. Finally, the conclusion will be given in Section 4.

2 Method Total energy calculations are performed using the full-potential linearized augmented plane wave (FP-LAPW) method as implemented in the WIEN2K code [12]. The exchange and correlation effects were treated using the GGA [4]. We expand the basis function up to $R_{MT}K_{MAX} = 9$ (R_{MT} is the muffin-tin radii, K_{MAX} is the maximum modulus for the reciprocal lattice vectors). The maximum value of partial waves inside atomic sphere is $l_{max} = 10$. Fully relativistic approximation is used for core electrons, and scalar relativistic approximation is used for valence electrons. Muffin-tin radii (R_{MT}) of 2.3 Bohr for all atoms. For the rocksalt phase, we have used a $11 \times 11 \times 11$ k-points mesh of Monkhorst-Pack (MP) [13].

For the dynamical properties we apply the GGA in a plane wave basis. We have used Troullier and Martin norm-conserving pseudopotentials [14], as implemented in the PWscf code [15]. The electron wave functions were expanded with a plane wave basis set with a kinetic energy of 80 Ry, and an energy cutoff of 500 Ry were included for the charge density. The k-space integration on the Brillouin zone (BZ) for the self-consistent calculations was calculated with a $8 \times 8 \times 8$ MP mesh. The lattice dynamics properties are calculated using the density functional perturbation theory [16], in particular, an $4 \times 4 \times 4$ q-points mesh of MP was used. These matrices were then Fourier interpolated to obtain the phonon dispersion curves.

3 Results and discussions The calculated total energies are fitted with the Murnaghan's equation of states [17], to obtain structural parameters. The calculated structural parameters for the ground state phases, namely the equilibrium lattice parameter a, and the bulk modulus B, are given in Table 1, with available experimental data and theoretical values. Comparing our results with data of experimental measurements [19], we find very good agreement. The rather relative weak overestimation of the lattice parameters is a well-known feature of the GGA.

Table 2 shows the calculated band gap energies of the NaX compounds in their ground state B1 phase within the Perdew–Burke–Ernzerhof approximation (GGA) [4]. Our calculated direct band gaps show the well-known underestimation of excitation energies of the GGA formalism as compared to experiment [7].

To overcome this band-gap-problem, we calculate the band gaps of the NaX compounds within the Engel–Vosko (EV) approximation [23], which is known to give – generally – large band gap compared to GGA. The calculated band gaps are given in Table 2. It is clear that the EV approximation opens the band gaps but it remains still smaller than the experimental one.

We decide further to improve the calculated band gaps of NaF, NaCl, NaBr, and NaI with respect to the EV approximation by adding a calculation using the modified Becke–Johnson (mBJ) exchange potential [24] within the GGA approximation.

The mBJ has been shown to give much more accurate band gaps than other functionals in a wide variety of materials [25–26], and compete in accuracy with expensive hybrid and GW methods.

Table 1 Calculated lattice parameter a, and the bulk modulus B of the rocksalt compounds NaF, NaCl, NaBr, and NaI compared to theoretical and experimental data.

		a (Å)	B (GPa)
NaF	present cal. FP-LAPW	4.695	45.49
	present cal. pseudopotential	4.693	45.10
	theory	4.707[a]	44.6[a]
	exp.	4.63[b]	46.5[c]
NaCl	present cal. FP-LAPW	5.701	24.18
	present cal. pseudopotential	5.695	23.96
	theory	5.698[a]	23.4[a]
	exp.	5.64[b]	24.0[c]
NaBr	present cal. FP-LAPW	6.059	19.92
	present cal. pseudopotential	6.023	19.60
	theory	6.02[d]	19.36[d]
	exp.	5.97[b]	19.9[c]
NaI	present cal. FP-LAPW	6.526	15.62
	present cal. pseudopotential	6.528	15.30
	theory		14.7[e]
	exp.	6.48[b]	15.1[c]

[a]Ref. [18].
[b]Ref. [19].
[c]Ref. [20].
[d]Ref. [21].
[e]Ref. [22].

Table 2 Calculated band gap energies of the Na-based alkali halides within various approximations (e.g., GGA, Engel–Vosko (EV), and mBJ) compared to experiment and theory. All energies are given in eV.

	E_g (GGA)	E_g (EV)	E_g (mBJ)	E_g (exp.)[a]	E_g (theory)
NaF	6.12	7.11	11.69	11.50	7.26[b],
NaCl	5.00	6.07	8.41	8.75	6.38[b], 6.45[c], 8.63[d], 8.65[e]
NaBr	4.05	5.36	6.74	7.10	5.84[b], 4.12[f]
NaI	3.60	4.62	5.49	5.90	4.37[b]

[a]Ref. [7].
[b]Ref. [5].
[c]Ref. [18].
[d]Ref. [27].
[e]Ref. [28].
[f]Ref. [21].

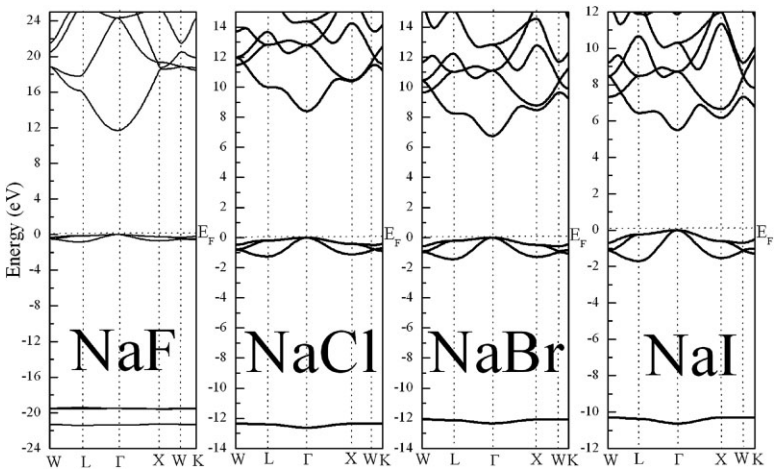

Figure 1 Electronic band structure of NaF, NaCl, NaBr, and NaI within the mBJ approximation.

The calculated band structures within the mBJ approximation for the alkali halides are given in Fig. 1. The calculated mBJ minimum energy gaps are 11.69, 8.41, 6.74, and 5.49 eV for NaF, NaCl, NaBr, and NaI, respectively.

Our mBJ band gaps result present perfect agreement with the experimental band gaps values [7] of 11.5 eV for NaF, 8.75 eV for NaCl, 7.1 eV for NaBr, and 5.9 eV for NaI.

The present mBJ band gap of NaCl agrees well with the recent GW [27, 28], but disagrees with the recent new hybrid functional (HSE03) [18] calculations.

We note that in all cases, the minimum energy gap is direct at the Γ point as found from the EV approximation; whereas earlier DFT calculations [5–6] exhibit the well-known severe underestimation of energy gaps. Furthermore the qualitative features in these band structures are found to be very similar. For example, the lowest valence band originates mainly from the halogen X (F, Cl, Br, I)-s orbital; while the VBM have a strong X-p character with a very weak admixture of Na-p states, making these compounds as strong ionic materials (see for instance partial density of states (PDOS) of NaCl, Fig. 2).

The calculated static properties, using pseudopotential and GGA, are given in Table 1. We also notice good agreement for structural properties with the present FP-LAPW calculations and experiment [19].

The calculated phonon dispersion curves of NaF, NaCl, NaBr, and NaI along the principal symmetry directions of the Brillouin zone are displayed in Fig. 3, and compared with neutron diffraction data [29–32]. Projected phonon densities of states (PPDOS) are given in Fig. 4. The calculated phonon frequencies resulting from the high symmetry points of the BZ are listed in Table 3. The agreement with the experiment is excellent for all compounds, which gives confidence in the predictive power of the present calculation. Moreover the present parameter-free calculations stand therefore, as reliable predictions for the full phonon curves of the NaX compounds.

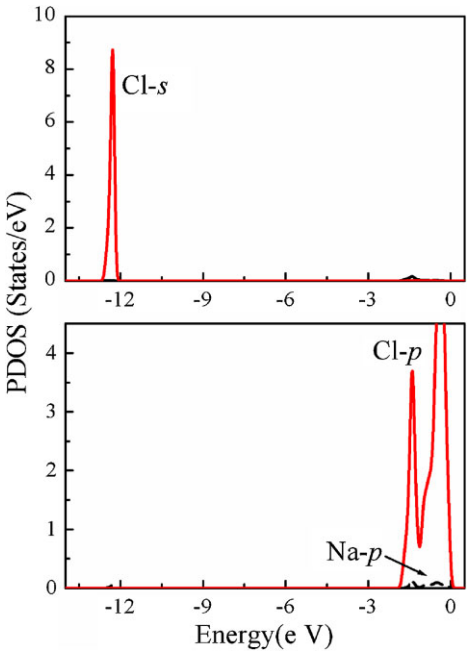

Figure 2 Partial density of states (PDOS) of NaF, NaCl, NaBr, and NaI.

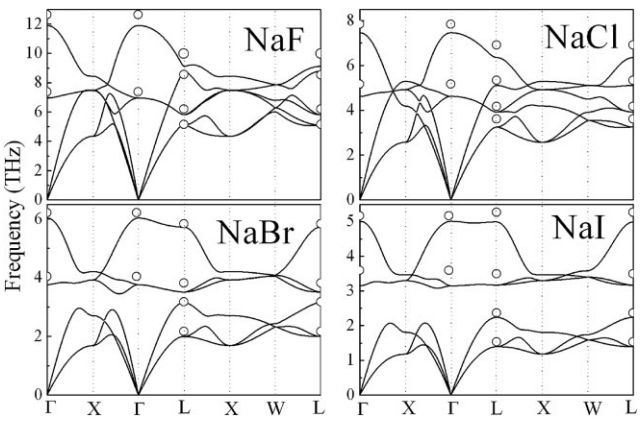

Figure 3 Phonon band structure of NaF, NaCl, NaBr, and NaI.

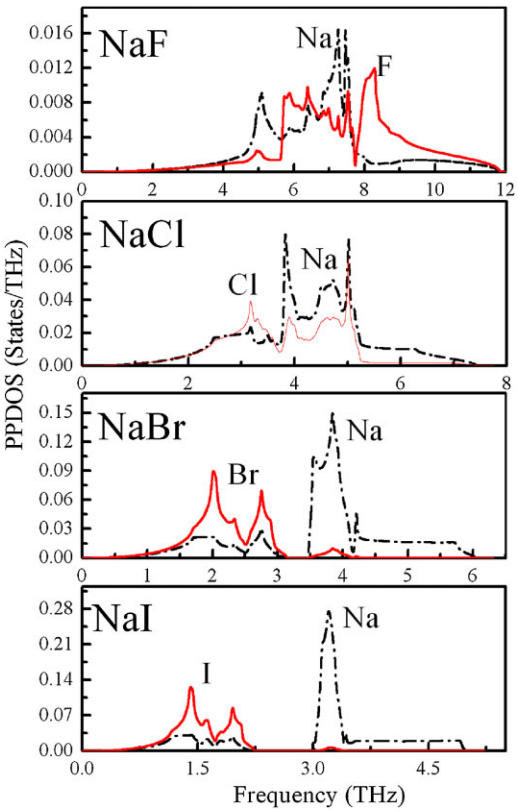

Figure 4 Partial phonon density of states (PPDOS) of NaF, NaCl, NaBr, and NaI. Dashed line for Na atom, red solid line for halogen X (F, Cl, Br, I) atoms.

In Table 3 we compare the calculated high-frequency dielectric constant $\varepsilon(\infty)$ of the NaX compounds with experimental values [33]. Once again our theoretical results for $\varepsilon(\infty)$ are in very good agreement with experiment. In comparison, other semiconductors compounds have much higher high-frequency dielectric constant such as Si (11.4 [35]), AlAs (8.16 [36]) where $\varepsilon(\infty)$ usually decreases with increasing ionicity.

The transverse Born effective charge $Z^{B}(\kappa)$ represents the charge of the κth ion interacting with the microscopic electric field. $Z^{B}(\kappa)$ is also referred to as dynamic effective charge as distinct from the static effective charge that results from the static transfer of the electron from cation to the anion when a crystal is formed. The acoustic sum rule requires that effective charge of the cation and anion are equal with opposite sign: $Z^{B}(\mathrm{Na}) = -Z^{B}(\mathrm{X})$. Values of the calculated Born effective charge of the Na-based alkali halides are listed in Table 3. Our results for $Z^{B}(\kappa)$ are in good agreement with the available experimental values. From Table 3, it is obvious that the calculated Born effective charge obtained for the NaX compounds are quite close to their nominal ionic charge. This is in agreement with the intuitive picture of these systems being highly ionic in nature.

The general shape of phonon dispersion curves in lighter anionic NaF and NaCl and heavier anionic NaBr and NaF are similar. Particularly there is no gap between the acoustic and the optical phonon modes in NaF and NaCl; whereas the acoustic and optical phonons are separated by a gap of ~0.33 THz for NaBr and ~0.77 THz for NaI. This is due to the considerable overlap between longitudinal acoustic (LA), and longitudinal optical (LO) phonon branches in NaF and NaCl; whereas the LA and LO phonon branches in NaBr and NaI does not cross. The energetical overlap is caused by the almost identical mass of N and F, atoms and N and Cl atoms.

Moreover the LA, and transverse optical (TO) phonon modes for NaF and NaCl and TO phonon modes for NaBr and NaI show strong flatness along a large part of the BZ. Due to this flatness, we observe very sharp peaks in the PPDOS (7.35 THz for NaF, 3.83 THz, and 8.01 THz for NaCl, 3.86 THz for NaBr, and 3.21 THz for NaI).

The calculated LO–TO splitting at the zone-center is, respectively, 4.94, 2.84, 2.27, and 1.86 THz for NaF, NaCl, NaBr, and NaI, which compare well with the measured

Table 3 Calculated high-dielectric function $\varepsilon(\infty)$, Born effective charges (Z^{*}), and phonon frequencies of alkali halides NaF, NaCl, NaBr, and NaI compounds compared to experimental data.

		$\varepsilon(\infty)$	Z^{*}(Na)	Z^{*}(X)	Γ_{LO}	Γ_{TO}	L_{LO}	L_{TO}	L_{LA}	L_{TA}
NaF	present cal.	1.85	1.019	−1.021	6.95	11.90	5.10	5.81	8.78	9.12
	exp.	1.74[a]	1.02[b]		7.385[c]	12.65[c]	5.145[c]	6.19[c]	8.543[c]	9.98[c]
NaCl	present cal.	2.47	1.105	−1.110	4.62	7.46	3.25	3.92	5.11	6.35
	exp.	2.33[a]	1.12[b]		5.172[d]	7.83[d]	3.613[d]	4.168[d]	5.332[d]	6.907[d]
NaBr	present cal.	2.79	1.141	−1.189	3.76	6.030	2.00	3.15	3.51	5.72
	exp.	2.60[a]			4.040[e]	6.220[e]	2.160[e]	3.180[e]	3.810[e]	5.830[e]
NaI	present cal.	3.35	1.207	−1.28	3.15	5.01	1.39	2.24	3.17	5.00
	exp.	3.01[a]			3.600[f]	5.170[f]	1.530[f]	2.360[f]	3.500[f]	5.270[f]

[a]Ref. [33].
[b]Ref. [34].
[c]Ref. [30].
[d]Ref. [31].
[e]Ref. [32].
[f]Ref. [33].

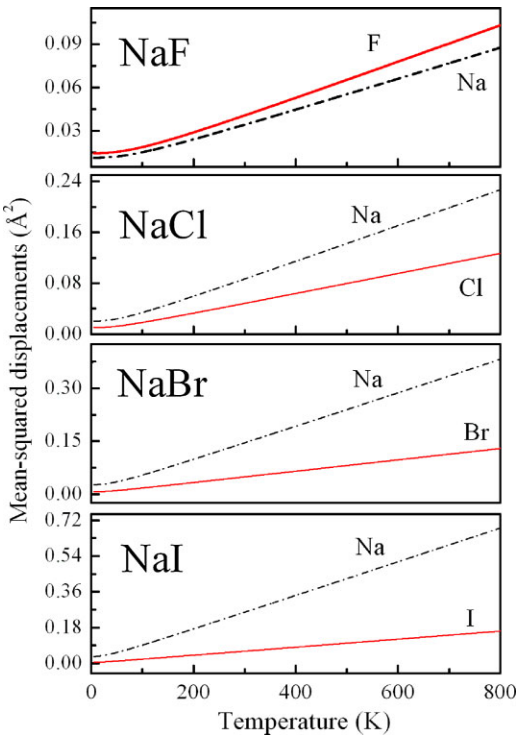

Figure 5 Mean-squared displacements versus temperature of NaF, NaCl, NaBr, and NaI. Dashed line for Na atom, red solid line for halogen X (F, Cl, Br, I) atoms.

LO–TO splitting of 5.26 THz for NaF [23], 2.66 THz for NaCl [24], 2.18 THz for NaBr [25], and 1.57 THz for NaI [26]. The large splitting of TO and LO modes at the zone center is a characteristic behavior for ionic crystals.

With the calculated phonon density of state, we are able to determine the thermodynamic properties of the NaX compounds using the quasi-harmonic approximation [37].

The mean-squared displacements versus temperature for the NaX compounds are plotted in Fig. 5. For NaF, we underline that Na and F atoms show small vibrational amplitudes difference, reflecting the small mass mismatch between Na and F atoms. While for NaCl, NaBr, and NaI, N atoms show strong vibrational amplitude as compared to X atoms. The vibrational amplitude of the X atoms decreases strongly with the increasing mass, according to the sequence NaF → NaCl → NaBr → NaI.

The variation of the heat capacity with temperature for the NaX compounds is illustrated in Fig. 6. The heat capacity increases strongly with temperature when the temperature is $T < 200$ K. For $T > 400$ K the heat capacity increases slowly with temperature and gradually approaches the Dulong–Petit limit ($\sim 50\,\mathrm{J\,mol^{-1}\,K}$) owing to the anharmonic approximations of the Debey model.

For NaF and NaCl compounds, the heat capacity originates principally from F and N acoustic modes in NaF, and from Na-Acoustic modes and with relatively small contribution from Cl-acoustic modes in NaCl. However for the heavier anionic NaBr and NaI compounds, the heat capacity originate principally from Na-optical modes and Br-Acoustic modes for NaBr; while the heat capacity originates principally from Na-optical modes and Ir-Acoustic modes for NaI.

4 Conclusions In summary we have investigated from first-principles calculation structural, optical, dynamical, and thermodynamic properties of alkali halides NaF, NaCl, NaBr, and NaI. Ground-state parameters, such as the lattice

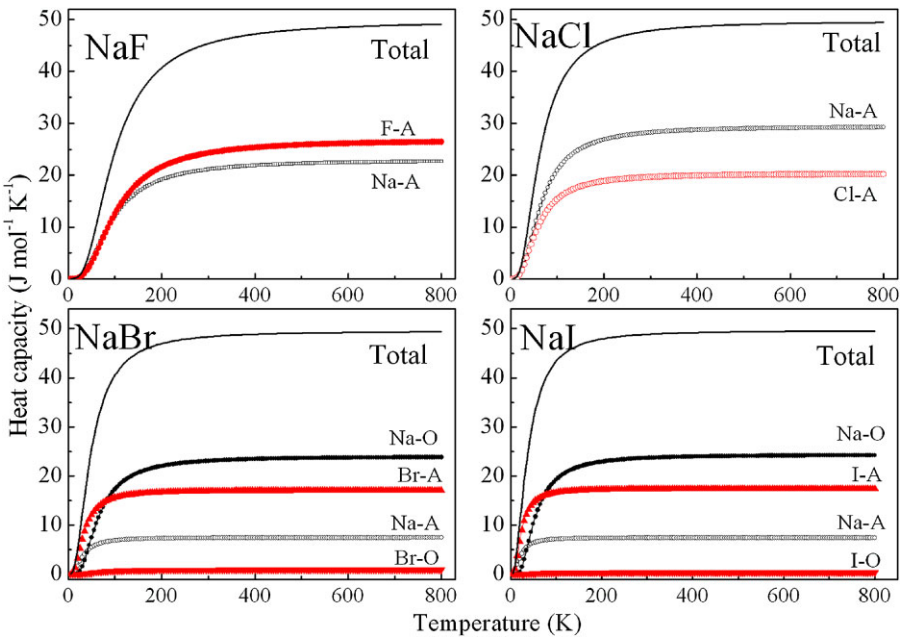

Figure 6 Heat capacity C_v of NaF, NaCl, NaBr, and NaI as a function of temperature.

constant and the bulk modulus were calculated using the FP-LAPW method. A linear-response approach within the *ab-initio* plane wave pseudopotential method was used to derive the Born effective charge, the high-frequency dielectric constants, phonon dispersions, and phonon density of states. We have highlighted the main features of the predicted phonon dispersion curves of the Na-alkali halides. Based on the results of these calculations, we further employed quasiharmonic approximation to calculate the temperature dependence of mean-squared displacement, and heat capacity.

References

[1] E. Madelung, Phys. Z. **19**, 524 (1918).
P. O. Ewald, Ann. Phys. (Leipzig) **64**, 253 (1921).
[2] W. Kohn and L. J. Sham, Phys. Rev. **140**, A1133 (1965).
[3] J. P. Perdew and Y. Wang, Phys. Rev. B **45**, 13244 (1992).
[4] J. P. Perdew, K. Burke, and M. Ernzerhof, Phys. Rev. Lett. **77**, 3865 (1996).
[5] J. Li, C-g. Duan, Z-q. Gu, and D-s. Wang, Phys. Rev. B **57**, 2222 (1998).
[6] C. R. Gopikrishnan, D. Jose, and A. Datta, AIP Adv. **2**, 012131 (2012).
[7] F. C. Brown, C. Gähwiller, H. Fujita, A. B. Kunz, W. Scheifley, and N. Carrera, Phys. Rev. B **2**, 2126 (1970).
[8] R. K. Singh and M. P. Verma, Phys. Rev. B **2**, 4288 (1970).
[9] A. N. Basu and S. Sengupta, Phys. Rev. B **8**, 2982 (1973).
[10] R. K. Singh and K. Chandra, Phys. Rev. B **14**, 2625 (1976).
[11] V. V. S. Nirwal and R. K. Singh, Phys. Rev. B **20**, 5379 (1979).
[12] P. Blaha, K. Schwarz, G. K. H. Madsen, D. Kvasnicka, and J. Luitz, Wien2k, An Augmented Plane Wave Program for Calculating Crystal Properties (Vienna University of Technology, Vienna, Austria, 2001).
[13] H. J. Monkhorst and J. D. Pack, Phys. Rev. B **13**, 5188 (1976).
[14] N. Troullier and J. L. Martin, Phys. Rev. B **43**, 1993 (1991).
[15] S. Baroni, A. DalCorso, S. de Gironcoli, and P. Giannozzi, http://www.pwscf.org.
[16] S. Baroni, S. de Gironcoli, A. DalCorso, and P. Giannozzi, Rev. Mod. Phys. **73**, 515 (2001).
[17] F. D. Murnaghan, Proc. Natl. Acad. Sci. USA **30**, 244 (1944).
[18] J. Paier, M. Marsman, K. Hummer, G. Kresse, I. C. Gerber, and J. G. Ángyán, J. Chem. Phys. **124**, 154709 (2006).
[19] W. J. Tropf, M. E. Thomas, and T. J. Harris, in: Handbook of Optics. 2nd ed., edited by M. Bass (McGraw-Hill, New York, 1995), Vol. 2, chap. 33.
[20] R. W. Roberts and C. S. Smith, J. Phys. Chem. Solids **31**, 619 (1970).
C. S. Smith and L. S. Cain, J. Phys. Chem. Solids **36**, 205 (1975).
[21] R. Ping, D. H. Yong, Z. J. Xi, and D. Ning, Chin. Phys. Lett. **1**, 216 (2008).
[22] B. Xu, Q. Wang, and Y. Tian, Sci. Rep. **3**, 3068 (2013).
[23] E. Engel and S. H. Vosko, Phys. Rev. B **47**, 13164 (1993).
[24] F. Tran and P. Blaha, Phys. Rev. Lett. **102**, 226401 (2009).
[25] D. Koller, F. Tran, and P. Blaha, Phys. Rev. B **83**, 195134 (2011).
[26] J. A. Camargo-Martinez and R. Baquero, Phys. Rev. B **86**, 195106 (2012).
[27] F. Bechstedt, K. Seino, P. H. Hahn, and W. G. Schmidt, Phys. Rev. B **72**, 245114 (2005).
[28] A. Kaur, E. R. Ylvisaker, D. Lu, T. A. Pham, G. Galli, and W. E. Pickett, Phys. Rev. B **87**, 155144 (2013).
[29] W. J. L. Buyeres, Phys. Rev. **153**, 923 (1967).
[30] G. Raunio, L. Almquist, and R. Stedman, Phys. Rev. **178**, 1496 (1969).
[31] J. S. Reid, T. Smith, and W. J. L. Buyeres, Phys. Rev. B **1**, 1833 (1970).
[32] R. A. Cowley, W. Cochran, B. N. Brockhouse, and A. D. B. Woods, Phys. Rev. **131**, 1630 (1963).
[33] R. P. Lowndes and D. H. Martin, Proc. R. Soc. A **308**, 473 (1969).
[34] M. Born and K. Huang, Dynamical Theory of Crystal lattices, 2nd ed. (Clarendon, Oxford, 2007).
[35] H. H. Li, J. Chem. Phys. Ref. Data **9**, 561 (1980).
[36] R. E. Fern and A. Onton, J. Appl. Phys. **42**, 3499 (1971).
[37] The QHA code has been written and developed by E. I. Isaev, https://qe-forge.org.

